ISSN: 2414-1895 DOI: 10.6919/ICJE.202411_10(11).0017

Study on the Optimization of Ultrasonic Milling Parameters for 7075 Aluminum Alloy

Yi Huang[1], Qingyun Dong[2,*], Yipu Bian[1], Xin Zhang[1], Chong Li[1], Shaokun Luo[1]

[1] School of Mechanical Engineering, Tianjin University of Technology and Education, Tianjin 300222, China

[2] Engineering Training Center, Tianjin University of Technology and Education, Tianjin 300222, China

[*]Corresponding author: Qingyun Dong, E-mail address: 13752680350@163.com

Abstract

In order to investigate the impact of various milling parameters on the milling force during the ultrasonic vibration-assisted milling process of 7075 aluminum alloy, orthogonal experiments were designed. The experimental data indicated that selecting a higher spindle speed, a lower feed rate, and a smaller milling depth could effectively reduce the milling force. Through analysis, the optimal milling parameter combination was determined to be: n=5500 r·min-1, vf=600 mm/min, and ap=0.2 mm. Furthermore, by measuring the surface roughness of the machined workpieces, it was found that the milling depth, spindle speed, and feed rate affect the surface roughness in descending order, further validating the effectiveness of the obtained optimal milling parameters.

Keywords

Ultrasonic Vibration-Assisted Milling; 7075 Aluminum Alloy; Parameter Optimization.

1. Introduction

In the current aerospace and automotive manufacturing industries, 7075 aluminum alloy is highly favored for its high strength and excellent mechanical properties. However, the high hardness and thermal sensitivity issues during the machining process of this material pose challenges to traditional milling processes [1-2]. To improve the machining efficiency and surface quality of the workpiece, ultrasonic milling technology has emerged, which effectively reduces cutting force and cutting temperature by introducing ultrasonic vibration during the cutting process, thus improving the surface integrity of the workpiece [3].

In the study of ultrasonic-assisted machining, researchers have found that appropriate ultrasonic amplitude and frequency can effectively reduce surface roughness and improve the surface hardness and fatigue life of the workpiece [4-5]. Zhao Chongyang [6] and others found that ultrasonic milling can also form micro-structures on the workpiece surface, which not only improve the wettability of the workpiece but also enhance its fatigue resistance and corrosion resistance. Mohammad L [7] and others found that when ultrasonic tools are used for milling CFRP, fiber pull-out is eliminated. In addition, the surface roughness is reduced by about 15%. At the same time, micro-structures are generated on the surface of titanium alloy workpieces using the harmonic motion of end mills.

In summary, ultrasonic milling technology has broad application prospects in the field of 7075 aluminum alloy processing. It can not only improve the processing efficiency and quality, but also expand the application range of aluminum alloy materials. In this study, the orthogonal experiment of ultrasonic milling for 7075 aluminum alloy was carried out to explore the influence of cutting factors on cutting force and optimize the process parameters.

ISSN: 2414-1895 DOI: 10.6919/ICJE.202411_10(11).0017

2. Experiment

2.1 Experimental Materials

In this experiment, 7075 aluminum alloy was selected for the workpieces, with dimensions of 100mm × 80mm × 40mm. The physical properties are shown in Table 1, and the chemical composition is presented in Table 2.

Table 1. Main physical properties of 7075 aluminum alloy

Tensile strength Mpa	0.2% Yield strength Mpa	Elastic modulus Gpa	Hardness HB	Density g/cm^3	Poisson's ratio
524	455	71	150	2.81	0.33

Table 2. Chemical composition of 7075 aluminum alloy

Si	Fe	Cu	Mn	Mg	Cr	Zn	Ti
0.4	0.5	1.2-2.0	0.3	2.1-2.9	0.18-0.28	5.1-6.1	0.2

2.2 Experimental Setup

In the experiment, a S56 vertical machining center produced by Makino Machine Tools Co., Ltd. was selected for the machining operation. The milling cutter used was a 6mm four-flute cemented carbide end mill with a helix angle of 35°. The force measurement system consists of a force transducer, charge amplifier, data acquisition system, and a computer, all manufactured by Kistler Instruments of Switzerland, with the model number being type 9257B. The charge amplifier, model 5070, is used to amplify the three-component signal data of the force platform through multiple channels. The data acquisition system, model 5697A1, is responsible for collecting the force data. Finally, a computer equipped with Dyon Ware software allows for the setting of time and frequency of the collected signals on the terminal device, real-time display of the force platform data during operation, and data saving and subsequent processing after the force measurement process is completed. The ultrasonic vibration device is composed of an ultrasonic tool holder and an ultrasonic intelligent generator. The experiment was conducted with the assistance of ultrasonic vibration, with the ultrasonic power set at 70%, frequency at 19,000 Hz, and amplitude at 3μm. The experimental platform and equipment connections are shown in Figure 1.

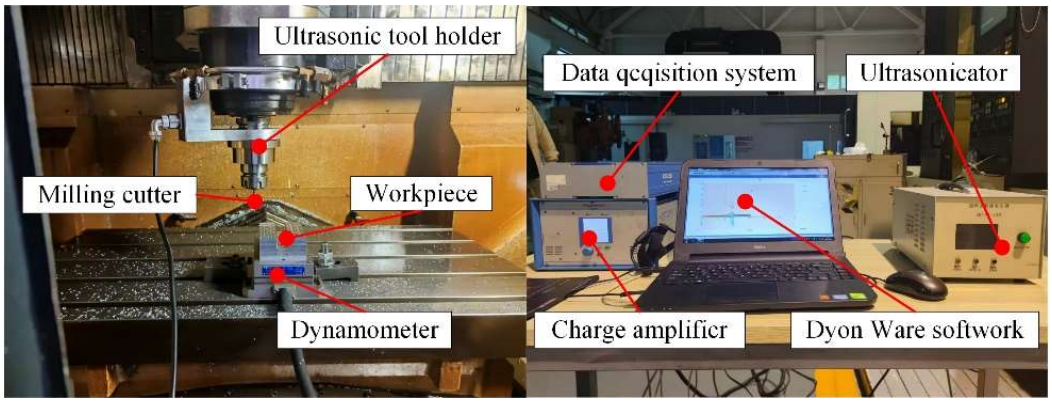


Figure 1. 7075 Aluminum Alloy Milling Experimental Platform

2.3 Experimental Scheme

In order to investigate the influence of milling parameters on the milling force of 7075 aluminum alloy and to determine the optimal combination of milling parameters, orthogonal milling experiments were conducted on 7075 aluminum alloy. A three-factor, four-level orthogonal

ISSN: 2414-1895 DOI: 10.6919/ICJE.202411_10(11).0017

experimental method was used, with the three factors being spindle speed, feed rate, and cutting depth. Each factor had four machining parameters set as the four levels in the orthogonal experiment. The factor level table is shown in Table 3.

Table 3. Factor level table

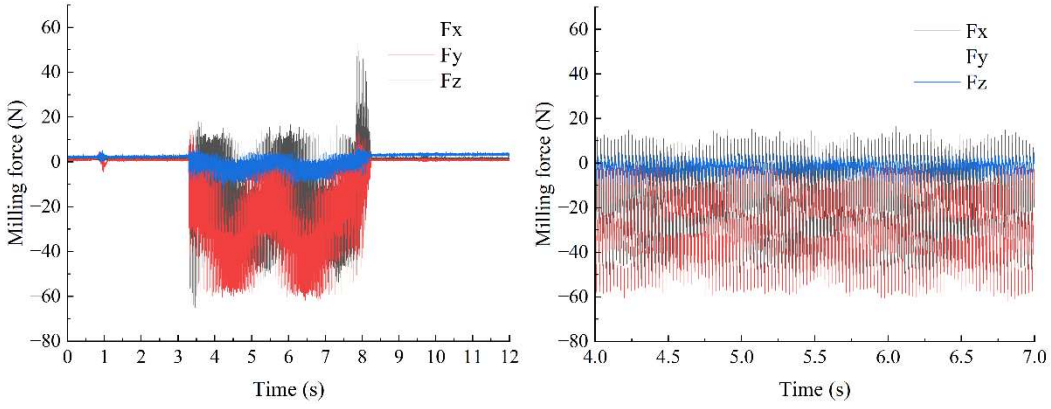
	n (r/min)	V_f(mm/min)	a_p (mm)
1	1000	200	0.2
2	2000	400	0.4
3	3000	600	0.6
4	4000	800	0.8

3. Results and Analysis

3.1 Results

The results of the orthogonal experiment are presented in Table 4. Through the data acquisition system, the milling forces in three directions were recorded on the computer and processed using software to generate a curve chart of the milling force over time, as shown in Figure 2, which displays the time-domain graph of the milling force under specific parameter settings. Figure 2(b) is an enlarged view of a particular section. It can be observed from Figure 2 that the data points of the milling force are relatively concentrated. To facilitate a more intuitive and convenient analysis of these measured milling force data, during the stable period of the milling process, we used the bilateral peak detection method, selected 100 peak values, and calculated their average value as the representative milling force for that set of parameters. The milling force data under all parameters were selected using the same method. Subsequently, the resultant milling force was calculated according to Equation (1), and the calculation formula is as follows:

$$F = \sqrt{F_x^2 + F_y^2 + F_z^2} \tag{1}$$



(a)Time domain diagram (b) Partial enlargement

Figure 2. Milling force time domain diagram.

In order to further verify the impact of milling parameters on the machining of 7075 aluminum alloy, we also conducted measurements of the workpiece's surface morphology and roughness. Figure 3 shows the surface morphology of the workpiece as seen under a white light interferometer.

ISSN: 2414-1895 DOI: 10.6919/ICJE.202411_10(11).0017

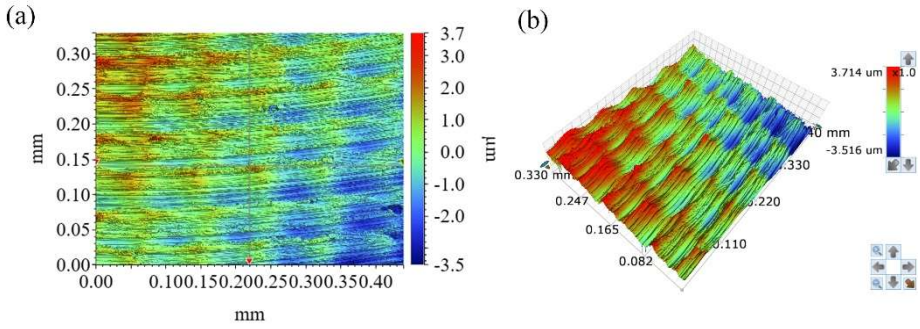


Figure 3. Surface morphology of workpiece: (a) two-dimensional morphology (b) three-dimensional morphology.

Table 4. Orthogonal experimental results

No.	n	v_f	a_p	Result				
	(r·min^{-1})	(mm·min^{-1})	(mm)	F_x	F_y	F_z	F	Ra
1	2500	300	0.2	17.7	28.26	2.18	33.42	0.854
2	2500	400	0.4	45.58	57.03	8.66	73.52	0.878
3	2500	500	0.6	59.19	76.32	20.36	98.71	1.04
4	2500	600	0.8	78	108.71	31.32	137.41	1.13
5	3500	300	0.4	35.77	35.08	6.13	50.47	0.807
6	3500	400	0.2	22.02	28.18	1.15	35.78	0.862
7	3500	500	0.8	70.67	80.56	28.54	110.9	0.934
8	3500	600	0.6	60.75	79.76	20.14	102.26	0.947
9	4500	300	0.6	61.64	58.67	19.42	87.28	1.97
10	4500	400	0.8	63.68	60.62	16.39	80.43	0.903
11	4500	500	0.2	65.3	57.82	19.55	89.38	0.836
12	4500	600	0.4	39.58	45.13	6.76	60.41	0.895
13	5500	300	0.8	51.23	46.6	21.11	72.4	0.853
14	5500	400	0.6	44.5	43.14	10.1	62.8	0.814
15	5500	500	0.4	38.64	39.5	5.97	55.58	0.841
16	5500	600	0.2	26.07	28.15	1.11	38.38	0.804

3.2 Analysis

- Milling Force

Based on the data from the orthogonal experiment, we conducted an extreme difference analysis of the milling force, and the results are summarized in Table 5. The extreme difference in Table 5 refers to the difference between the maximum and minimum values of the $\overline{K}$ values under each single factor (including spindle speed, feed rate, and milling depth). The optimal level is the level where the corresponding variable is minimized. The primary and secondary influence order of each factor is arranged from largest to smallest based on the extreme difference. The analysis results in Table 5 show that for the X- axis milling force, the order of influencing factors is milling depth > feed rate > spindle speed, with the optimal parameter combination being A1B1C1, which means a spindle speed of 2500 r·min-1, feed rate of 300 mm·min-1, and milling depth of 0.2mm. For the Y- axis milling force, the order of influencing factors is milling depth > spindle speed > feed rate, with the optimal

ISSN: 2414-1895 DOI: 10.6919/ICJE.202411_10(11).0017

parameter combination being A4B4C1, which means a spindle speed of 5500 r·min-1, feed rate of 600 mm·min-1, and milling depth of 0.2mm. For the Z- axis milling force, the order of influencing factors is the same as for the Y- axis, but the optimal parameter combination is also A4B4C1. For the resultant milling force, the order of influencing factors is the same as for the Y- axis, but the optimal parameter combination is A1B1C1, which means a spindle speed of 2500 r·min-1, feed rate of 300 mm·min-1, and milling depth of 0.2mm.

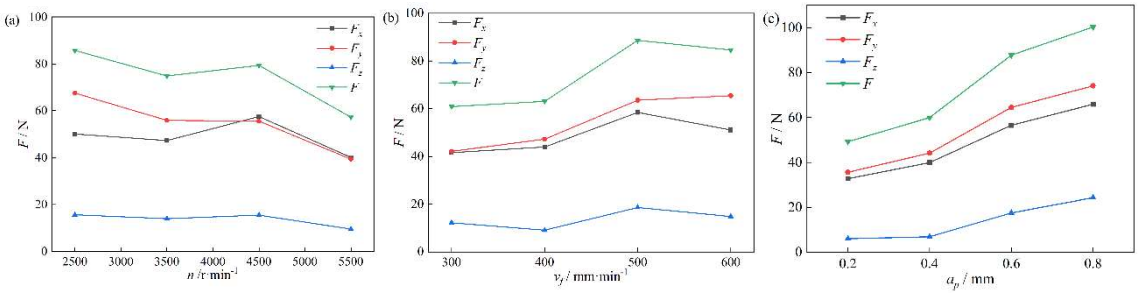


Figure 4. The influence of milling parameters on milling force: (a)Spindle speed; (b) Feed speed; (c) Milling depth

Table 5. Milling force range analysis results

		n/(r·min^{-1})	v_f/(mm·min^{-1})	a_p/mm
F_x	$\bar{K}_1$	50.12	41.59	32.77
	$\bar{K}_2$	47.30	43.95	39.89
	$\bar{K}_3$	57.55	58.45	56.52
	$\bar{K}_4$	40.11	51.10	65.90
	Range	10.01	16.86	33.13
F_y	$\bar{K}_1$	67.58	42.15	35.60
	$\bar{K}_2$	55.90	47.24	44.19
	$\bar{K}_3$	55.56	63.55	64.48
	$\bar{K}_4$	39.35	65.44	74.12
	Range	28.23	23.29	38.52
F_z	$\bar{K}_1$	15.63	12.21	6.00
	$\bar{K}_2$	13.99	9.08	6.88
	$\bar{K}_3$	15.53	18.61	17.50
	$\bar{K}_4$	9.57	14.83	24.34
	Range	6.06	9.53	18.34
F	$\bar{K}_1$	85.77	60.89	49.24
	$\bar{K}_2$	74.85	63.13	60.00
	$\bar{K}_3$	79.37	88.64	87.76
	$\bar{K}_4$	57.29	84.61	100.29
	Range	28.48	27.75	51.05

ISSN: 2414-1895 DOI: 10.6919/ICJE.202411_10(11).0017

In order to explore the impact of different milling parameters on the milling force of 7075 aluminum alloy under ultrasonic vibration assistance, the influence of each processing parameter on the milling forces Fx, Fy, Fz, and the resultant force F was plotted according to Table 5 under three factors (spindle speed, feed rate, and milling depth). From Figure 2(a), it can be seen that as the spindle speed increases, Fx first increases and then decreases, reaching the maximum cutting force at 4500 r·min-1. Meanwhile, Fy, Fz, and the resultant force F all show a decreasing trend. When the spindle speed increases from 2500 r·min-1 to 5500 r·min-1, Fy decreases by 28.23N, a reduction of 41.8%, Fz decreases by 6.06N, a reduction of 38.8%, and the resultant force F decreases by 28.48N, a reduction of 33.2%. From Figure 2(b), it can be seen that as the feed rate increases from 300 mm·min-1 to 600 mm·min-1, Fy shows an increasing trend. The reason for the increase is that the feed direction set in the experiment is in the Y direction. As the feed rate increases, the amount of milling in the Y direction also gradually increases, so the cutting force will correspondingly become larger. Fx, Fz, and the resultant force F all show a stable increase as the feed rate increases from 300 mm·min-1 to 500 mm·min-1, but they all show a slight decrease when increased to 600 mm·min-1. However, overall, the cutting force will gradually increase with the increase of the feed rate. From Figure 4(c), it can be seen that as the milling depth increases from 0.2 mm to 0.8 mm, Fx, Fy, Fz, and the resultant force F all show an increasing trend. The reason for the increase is that with the increase of milling depth, the total amount of milling per unit time increases, which in turn leads to an increase in milling force.

Based on the analysis, using a higher spindle speed, a smaller feed rate, and a shallow milling depth can help reduce the milling force.

- Roughness

The analysis of the roughness measurements, as shown in Table 6, indicates that the factor with the greatest impact on the surface roughness of the workpiece is the milling depth, followed by the spindle speed, and then the feed rate. The optimal parameter combination is A4B4C1, which corresponds to a spindle speed of 5500 r·min-1, a feed rate of 600 mm·min-1, and a milling depth of 0.2 mm. This aligns with the influence hierarchy of the factors for the Y-axis, Z-axis, and the overall milling force.

Examining the values presented in Table 6, one can observe that there is a change with the escalation of the spindle speed, the roughness generally shows a decreasing trend. At a spindle speed of 2500 r·min-1, the roughness is 0.976μm, and when the spindle speed is increased to 5500 r·min-1, the roughness is reduced to 0.828μm. As the feed rate increases, the roughness first decreases and then increases, but ultimately shows an increasing trend. This is because the increase in feed volume leads to more total milling per unit time, which ultimately affects the surface quality of the workpiece. As the milling depth increases from 0.2mm to 0.8mm, the surface roughness of the workpiece shows a stable increasing trend, increasing from 0.839μm to 1.193μm, a 39.64% increase, which is also caused by the increase in the total amount of milling.

This further illustrates that in the milling of 7075 aluminum alloy, using a higher spindle speed, a smaller feed rate, and a smaller milling depth can reduce the milling force, thereby achieving better surface quality.

Table 6. Roughness range analysis results

		n/(r·min^{-1})	v_f/(mm·min^{-1})	a_p/mm
Ra	$\overline{K_1}$	0.976	1.121	0.839
	$\overline{K_2}$	0.888	0.864	0.855
	$\overline{K_3}$	1.151	0.912	0.955
	$\overline{K_4}$	0.828	0.944	1.193
	Range	0.323	0.257	0.354

ISSN: 2414-1895 DOI: 10.6919/ICJE.202411_10(11).0017

4. Conclusion

In this study, the optimization of milling parameters for 7075 aluminum alloy milling under ultrasonic vibration assistance was carried out. An orthogonal experiment was designed to investigate the impact of milling parameters on milling force and surface roughness. The range analysis method was used to determine the order of influence of each milling parameter on milling force and surface roughness, as well as the optimal combination of milling parameters. This study provides certain references for the milling process of 7075 aluminum alloy under ultrasonic vibration assistance. The research conclusions are as follows:

- The influence order of milling parameters on the X-axis milling force is milling depth > feed rate > spindle speed, on the Y-axis milling force is milling depth > spindle speed > feed rate, on the Z-axis milling force is milling depth > feed rate > spindle speed, and on the resultant milling force is milling depth > feed rate > spindle speed.
- The influence order of milling parameters on the surface roughness of the workpiece is milling depth > spindle speed > feed rate, with the optimal milling parameters being a spindle speed of 5500 $r \cdot min^{-1}$, a feed rate of 600 $mm \cdot min^{-1}$, and a milling depth of 0.2mm.

Acknowledgments

This work was supported by the Natural Science Foundation of Tianjin (Grant No. 22JCZDJC00740).

References

[1] Aishah Najiah Dahnel, Muhamad Ali Abdul Ghani, Natasha A. Raof, et al. Analysis of defects on machined surfaces of aluminum alloy (Al 7075) using imaging and topographical techniques[J]. International Journal of Metrology and Quality Engineering. 2022;13 (0):12-12.

[2] Lin H, Jin G, Luo S, Wang G, Li Z. Modified constitutive models and cutting finite element simulation of Ti-6Al-4V alloy at cryogenic[J]. Proceedings of the Institution of Mechanical Engineers, Part C: Journal of Mechanical Engineering Science. 2024;0(0).

[3] Li, Z., Ma, Y., Jin, G. et al. Research on the surface morphology of titanium alloy ultrasonic elliptical vibration cutting considering flank extrusion and material rebound[J]. Int J Adv Manuf Technol 134, 1487–1506 (2024).

[4] Chai Ning-Sheng, Zhang Min-Liang, Shi Chun-Guang, et al. Simulation Study on Ultrasonic Vibration Milling of 7075 Aluminum Alloy [J]. Agricultural Equipment & Vehicle Engineering, 2023, 61(01): 144-148.

[5] Qingqing Lü, Shuangming Yang, Liquan Yang, et al. Optimization Milling Force and Surface Roughness of Ti-6Al-4V Based on Ultrasonic-Assisted Milling (UAM): An Experimental Study. Micromachines[J]. 2023;14 (9):1699-1699.

[6] Zhao Chongyang, Lu Junyu, Wang Xiaobo, et al. Study on the Surface Wettability of High-Strength Aluminum Alloy by Ultrasonic Vibration-Assisted Milling [J]. China Mechanical Engineering, 2022, 33(16): 1912-1918+1927.

[7] Mohammad Lotfi, Ali Charkhian, Jafar Âkbari. Surface analysis in rotary ultrasonic-assisted milling of CFRP and titanium[J]. Journal of Manufacturing Processes. 2022;84 (0):174-182.